DNA replication fidelity in *Mycobacterium tuberculosis* is mediated by an ancestral prokaryotic proofreader

Jeremy M. Rock[#1], **Ulla F. Lang**[#2], **Michael R. Chase**[1], **Christopher B. Ford**[1,3], **Elias R. Gerrick**[1], **Richa Gawande**[1], **Mireia Coscolla**[4,5], **Sebastien Gagneux**[4,5], **Sarah M. Fortune**[#1,3,6], and **Meindert H. Lamers**[#2]

[1]Department of Immunology and Infectious Diseases, Harvard School of Public Health, Boston, Massachusetts, USA [2]MRC Laboratory of Molecular Biology, Cambridge, UK [3]The Broad Institute of MIT & Harvard, Cambridge, Massachusetts, USA [4]Swiss Tropical and Public Health Institute, Basel, Switzerland [5]University of Basel, Basel, Switzerland [6]The Ragon Institute of MGH, Harvard and MIT, Cambridge, Massachusetts, USA

[#] These authors contributed equally to this work.

Abstract

The DNA replication machinery is an important target for antibiotic development for increasingly drug resistant bacteria including *Mycobacterium tuberculosis*[1]. While blocking DNA replication leads to cell death, disrupting the processes used to ensure replication fidelity can accelerate mutation and the evolution of drug resistance. In *E. coli*, the proofreading subunit of the replisome, the ε-exonuclease, is essential for high fidelity DNA replication[2]; however, we find that it is completely dispensable in *M. tuberculosis*. Rather, the mycobacterial replicative polymerase, DnaE1, encodes a novel editing function that proofreads DNA replication, mediated by an intrinsic 3′-5′ exonuclease activity within its PHP domain. Inactivation of the DnaE1 PHP domain increases the mutation rate by greater than 3,000 fold. Moreover, phylogenetic analysis of DNA replication proofreading in the bacterial kingdom suggests that *E. coli* is a phylogenetic outlier and that PHP-domain mediated proofreading is widely conserved and indeed may be the ancestral prokaryotic proofreader.

In the model organism *E. coli*, DNA replication fidelity is determined by three main processes: nucleotide insertion fidelity by the DNA polymerase, removal of mis-incorporated nucleotides by the associated 3′-5′ proofreading exonuclease, and post-replicative mismatch repair (MMR), leading to the basal mutation rate of $\sim 10^{-10}$ mutations per base pair per generation[2]. Surprisingly, mycobacteria and all actinomycetes lack the

genes encoding the MMR system[3,4]. Whereas *E. coli* MMR mutants show ~100-1000 fold increased mutation rates, the basal mutation rate of mycobacteria remains roughly equivalent to that of wild-type *E. coli*[2,5].

In *E. coli*, DNA replication proofreading is performed by the 3′-5′ exonuclease ε encoded by the *dnaQ* gene[2]. The ε-exonuclease subunit associates with the DNA polymerase PolIIIα in *trans* and excises mis-inserted bases during DNA replication. Like *E. coli, M. tuberculosis* encodes an annotated *dnaQ* homologue (*Rv3711c;* Supplemental Figure 1) that has been assumed to play an important role in replication fidelity[6,7]. We hypothesized that *dnaQ* might play a dominant role in replication fidelity in mycobacteria. Surprisingly, however, deletion of *dnaQ* did not result in a mutation rate increase in mycobacteria as measured by fluctuation analysis (Figure 1A-B). Mycobacteria encode a second potential *dnaQ* homologue (*Ms4259;* Supplemental Figure 1). However, deletion of this second gene, either individually or in combination with the annotated *dnaQ* gene, did not increase the mutation rate (Figure 1B). In addition, while purified *M. tuberculosis* DnaQ has 3′-5′ DNA exonuclease activity (Supplemental Figure 2A-B), it does not stably associate with *M. tuberculosis* DnaE1 (DnaE1^{MTB}) (Supplemental Figure 2C), whereas *E. coli* DnaQ (ε) forms a tight complex with *E. coli* PolIIIα (PolIIIα^{EC}) (Supplemental Figure 2D).

These data suggest that mycobacteria use an alternative exonuclease to ensure replicative fidelity. While DnaE-type polymerases, including PolIIIα^{EC} and DnaE1^{MTB}, are thought to rely on proofreading provided in *trans* by the ε-exonuclease[2,8], it has been demonstrated *in vitro* that the DnaE polymerase from two thermophiles harbors an intrinsic 3′-5′ exonuclease activity in the Polymerase and Histidinol Phosphatase (PHP) domain[9,10]. The function of PHP domain exonuclease activity has remained unclear because the *Thermus* species also contain an annotated *dnaQ* homologue[8,9]. Given our finding that *dnaQ* does not significantly contribute to replication fidelity in mycobacteria (Figure 1A-B), we hypothesized that the PHP domain of DnaE1^{MTB} encodes an intrinsic exonuclease activity that is the primary source of proofreading in this pathogen.

In the thermophiles, PHP exonuclease activity depends on metal ion coordination by nine conserved amino acids within the PHP domain[9-11]. These amino acids are conserved in DnaE1^{MTB} (Figure 1C, Supplemental Figure 3) but mutated in PolIIIα^{EC} where exonuclease activity is lost[11]. To determine if DnaE1^{MTB} has exonuclease activity, we purified recombinant wild-type DnaE1^{MTB} and two mutants in which metal-coordinating residues were mutated (D23N or D226N) (Supplemental Figure 4A). Purified wild-type and mutant DnaE1^{MTB} showed similar gel filtration profiles (Supplemental Figure 4B) and similar folding and thermal stability as measured by circular dichroism (Supplemental Figure 4C-D). Using a real-time primer extension assay[11], we found that wild-type and PHP mutant DnaE1^{MTB} proteins also showed robust DNA polymerase activity (Figure 1D). Indeed, under saturating nucleotide concentrations, the V_{max} for DnaE1^{MTB} *in vitro* was faster than PolIIIα^{EC} (Figure 1E).

To determine if the PHP domain of DnaE1^{MTB} has exonuclease activity, we monitored cleavage of fluorescently labeled single-stranded DNA (ssDNA) oligos. Wild-type DnaE1^{MTB} shows clear 3′-5′ exonuclease activity (Figure 1F) but no 5′-3′ exonuclease

(Supplemental Figure 4E). In contrast, PHP mutant DnaE1^{MTB} proteins lack exonuclease activity (Figure 1F). In this assay, PHP-mediated exonuclease activity is distinct from that of the *E. coli* ε-exonuclease and appears to pause at sites of predicted secondary structure in the ssDNA (Figure 1F, data not shown).

To test the ability of DnaE1^{MTB} to excise mismatches during DNA synthesis *in vitro*, we performed primer extension assays using double-stranded (dsDNA) substrates containing either matched or mismatched 3′ primer termini. Wild-type DnaE1^{MTB} extends from all substrates with similar efficiency (Figure 1G-H). This activity does not appear to be mismatch extension because the use of a mismatched primer refractory to exonuclease activity cannot be extended by DnaE1^{MTB} (Supplemental Figure 5A). In contrast to wild-type DnaE1^{MTB}, the PHP mutants were unable to extend mismatched substrates (Figure 1G-H). The behavior of the PHP mutant DnaE1^{MTB} proteins is very similar to that of PolIIIα^{EC} in the absence of the ε-exonuclease, where almost no primer extension is observed (Figure 1G-H). Extension of a mismatched substrate could be rescued in the PHP mutants by addition of exogenous *E. coli* ε-exonuclease, suggesting that the defect in the ability of the PHP mutant DnaE1^{MTB} proteins to extend mismatched substrates is specific to their loss of exonuclease activity (Supplemental Figure 5B). These data demonstrate that DnaE1^{MTB} encodes an intrinsic 3′-5′ exonuclease activity that, at least *in vitro*, is capable of correcting mismatches.

We then assessed the importance of PHP-mediated exonuclease activity for DNA replication proofreading *in vivo*. Because *dnaE1* is an essential gene[12], we first determined the consequences of inducible overexpression of wild-type *dnaE1* or the PHP mutant alleles. Overexpression of wild-type *dnaE1* does not increase the mutation rate (Figure 2A-B). In contrast, overexpression of either *M. tuberculosis* or *M. smegmatis* PHP mutant *dnaE1* alleles led to a dose-dependent increase in the mutation rate (Figure 2A-B).

We then used an allele swapping system to replace the endogenous *dnaE1* allele with either the wild-type or PHP mutant *dnaE1* alleles. Both wild-type and PHP mutant *dnaE1* alleles could substitute for wild-type *dnaE1*, indicating that both were sufficient for viability (Figure 2C). However, while wild-type complemented strains grew normally, strains complemented with the PHP mutant alleles were severely attenuated for growth (Figure 2D). Because this growth defect precluded the use of fluctuation analysis to measure the mutation rate, we instead performed mutant accumulation assays and enumerated accumulation of mutations using whole genome sequencing. In a mutant accumulation assay, we found the basal mutation rate for *M. smegmatis* complemented with wild-type *dnaE1* to be ~4.5×10^{-10} mutations per base pair per generation, consistent with data from fluctuation analysis and previously published estimates (Table 1, Supplemental Figure 6)[13]. In contrast, the mutation rate in the absence of PHP exonuclease activity was ~1.0 to 1.7×10^{-6} mutations per base pair per generation or ~7 to 11 mutations per genome per generation, a ~2,300–3,700 fold increase over the wild-type rate (Table 1). The mutational spectra in both wild-type and the PHP mutant strains are notable for the relatively high frequency of insertion and deletion events[14], which is consistent with a lack of a functional MMR system in mycobacteria[4].

We hypothesize that the growth defect in the PHP mutants reflects either: 1) a defect in DNA polymerase function; and/or 2) the large increase in the mutation rate decreases strain fitness. Our data suggest that a defect in PHP mutant DNA polymerase function is unlikely to be an artifact of protein folding or stability issues (Figure 1D, Figure 2A-C, Supplemental Figure 4). Rather, the growth defect may be due to DNA replication stalling as a result of the relative inability of DnaE1 to extend from mis-incorporated nucleotides (Figure 1H). Alternatively, the growth defect could result from an increased mutation rate. In *E. coli*, the site-specific disruption of DnaQ (ε) proofreading is lethal but this lethality can be suppressed by overexpression of MutL or a PolIIIα[EC] anti-mutator allele, suggesting that an increased mutation rate alone can result in a significant fitness cost[15].

Thus, we find that the PHP domain of DnaE1, not *dnaQ*, is the major replicative exonuclease and a critical determinant of DNA replication fidelity in mycobacteria. Bacterial pathogens under rapidly changing selective pressures often inactivate MMR and acquire a selective advantage by becoming hypermutable[16]. Since *M. tuberculosis* does not encode homologues of the MMR system[3,4], we asked whether clinical *M. tuberculosis* strains increase their mutability through loss of PHP domain function or whether PHP domain-mediated proofreading serves a more essential function. Analysis of *dnaE1* sequences from ~1,700 clinical *M. tuberculosis* isolates revealed three missense SNPs found in ~3% of all isolates (Supplemental Figure 7A, Supplemental Table 3). By fluctuation analysis, we found one SNP (DnaE1 K95N) in a single clinical *M. tuberculosis* isolate that caused a small (3-fold) increase in the mutation rate; in no cases did PHP domain mutations fully abrogate PHP domain function (Supplemental Figure 7B). Thus, PHP domain-mediated proofreading may be essential for *M. tuberculosis* pathogenesis.

We next sought to determine the distribution of these two contrasting mechanisms of DNA replication fidelity, the PHP domain and the *E. coli*-like ε-exonuclease, in the bacterial kingdom (see Supplemental Table 4 for the ~2,000 bacterial species analyzed). All bacterial replicative DNA polymerases have a PHP domain[8]. Using conservation of all nine metal ion-coordinating residues as a proxy for an active exonuclease PHP domain, we categorized replicative DNA polymerases as either having an "active" or "inactive" PHP domain. In addition, each bacterial species was also queried for the presence of an *E. coli*-like ε-exonuclease homologue. Based on sequence alignments of ε homologues from *γ*-proteobacteria, an *E. coli*-like ε-exonuclease homologue was defined by the presence of a single domain protein containing a DEDDh-family exonuclease followed immediately by a clamp binding motif[17]. In a complementary analysis which produced concordant results, we defined *E. coli*-like ε homologues more broadly by homology to a hidden Markov model built from manually curated alignments of proteobacterial ε-exonucleases[18].

In agreement with a recent phylogenetic study of DNA PolIII α homologues[19], we find that the majority of replicative bacterial polymerases contain an active PHP exonuclease (Figure 3A-B). However, the majority of bacterial classes do not have an *E. coli*-like ε-exonuclease (Figure 3A-B). Putative ε-exonuclease homologues are distributed between two well-defined groups (Figure 3A), with only the higher scoring group showing all characteristics of an *E. coli*-like ε homologue. The lower scoring group, which includes the annotated *dnaQ* homologues in mycobacteria, appears to encode 3′-5′ exonucleases but lack distinguishing

characteristics of *E. coli* ε (Supplemental Table 5, data not shown). *E. coli*-like ε-exonucleases appear to exist uniquely within the α, β, and γ proteobacteria (Figure 3B, Supplemental Table 5)[11]. In a subset of bacteria, an ε-like exonuclease domain has been either inserted into the PHP domain of the replicative DNA polymerase (constituting the PolC family of polymerases) or fused to the N-terminus of a DnaE1-type DNA polymerase (Figure 3B)[19]. In contrast to previous observations that suggest DNA PolIII α homologues may coordinately utilize both PHP and ε-like exonuclease activity[19], we find that, though there are rare exceptions, broadly, the presence of an active PHP domain appears to be mutually exclusive with the presence of an *E.coli-like* ε-exonuclease or an ε-like exonuclease encoded within the polymerase (e.g. PolC). While these data do not preclude another role for the annotated ε homologues in DNA replication in species containing an active PHP domain, they suggest that the PHP domain is the most common replicative exonuclease in the bacterial kingdom and may be the ancestral prokaryotic proofreader.

Finally, bacterial DNA polymerases are active drug targets[1] but have not been successfully targeted by nucleoside analogs, which are commonly used to treat cancer and viral infections[20]. Nucleoside analogs mimic their physiological counterparts and are incorporated into DNA and/or RNA to inhibit cellular division and viral replication[20]. There have been efforts to use adenosine analogs to treat *M. tuberculosis* but with minimal success[21]. We reasoned that, in addition to imposing a severe fitness cost on its own (Figure 2D), inhibition of PHP domain-mediated proofreading might sensitize mycobacteria to nucleoside analogues. We first identified nucleoside analogs that specifically disrupt DNA synthesis mediated by PHP mutant DnaE1 *in vitro* (Figure 4A; data not shown), subsequently focusing on ara-A, a chain terminating adenosine analog that can be phosphorylated to its active form in *M. tuberculosis* by adenosine kinase[21]. Both wild-type and PHP mutant DnaE1 appear to incorporate ara-A at similar rates *in vitro* (Figure 4A). However, while wild-type DnaE1 efficiently removes incorporated ara-A, the PHP mutants remain blocked at sites of ara-A incorporation (Figure 4A). Consistent with these *in vitro* results, ara-A has no activity against mycobacteria containing wild-type *dnaE1* but is toxic to mycobacteria in which PHP activity is inhibited (Figure 4B), presumably as a result of inhibition of DNA replication. Disruption of DNA synthesis by PHP domain inhibition coupled with nucleoside analog treatment would represent a new mechanism of action for an antibiotic and a novel therapeutic option for drug-resistant *M. tuberculosis*.

Methods

Media

M. tuberculosis (H37Rv) or *M. smegmatis* (mc^{2}155) were grown at 37°C in Middlebrook 7H9 broth or 7H10 plates supplemented with the appropriate antibiotics.

Bacterial strains and plasmids

All *M. tuberculosis* strains are derivatives of H37Rv; all *M. smegmatis* strains are derivatives of mc^{2}155 with the exception of the protein production strain, which is a derivative of mc^{2}4517. Bacterial strains are listed in Supplemental Table 1. All plasmids generated in this study are listed in Supplemental Table 2.

Allele-swap experiments

dnaE1 plasmids were transformed into strain JR19 (*dnaE1:**Hyg dnaE1:**L5(Zeo) [Ms3178]*), plated on 7H10 plates supplemented with kanamycin, and incubated at 37°C for 4-5 days. Individual colonies were then patched to 7H10 plates containing either kanamycin or zeocin. Kanamycin resistant, zeocin sensitive colonies were scored as "allele-swap" (i.e. strains in which the transformed kanamycin-marked *dnaE1* plasmid replaced the zeocin-marked *dnaE1* plasmid at *attB*). Kanamycin resistant, zeocin resistant colonies were scored as "co-integrant" (i.e. strains in which the transformed kanamycin-marked *dnaE1* plasmid integrated adjacent to the zeocin-marked *dnaE1* plasmid at *attB*).

Mutant accumulation assay (MAA)

MAA strains were generated by transforming the allele-swap strain JR19 (*dnaE1:**Hyg dnaE1:**L5(Zeo) [Ms3178]*) with plasmid pJR23 (*dnaE1:**L5(Kan) [Ms3178]*), plasmid pJR161 (*dnaE1-D25N+silent:**L5(Kan) [Ms3178]*), or plasmid pJR87 (*dnaE1-D228N +silent:**L5(Kan) [Ms3178]*) and plating on 7H10+kanamycin plates. Plasmids pJR87 and pJR161 incorporated silent mutations flanking the PHP domain mutation to allow for unambiguous scoring of any reversion events. Resulting colonies were then re-streaked to singles on 7H10+kanamycin plates. Individual colonies were then again streaked to singles on a 7H10 plate and confirmed for allele-swap based on resistance to kanamycin and sensitivity to zeocin. The resulting patch from the 7H10 plate was used as the "time 0" strain isolate for the MAA. For each genotype, 12 MAA lines originated from single ~0.5 mm colonies isolated on 7H10 plates. Each line was streaked for single colonies on a 7H10 plate and incubated for 3-4 days (wild-type complemented) or 8 days (PHP mutant complemented). This procedure was then followed repeatedly for the desired number of passages.

Estimation of generations in a colony

The number of cells in a colony was determined by excising mc^{2}155 colonies of an average diameter of ~0.5 mm from agar plates, resuspending them in PBS+0.05% Tween-80, generating a single cell suspension by sonication, and plating dilutions on 7H10 plates. The average number of cells in a ~0.5 mm colony was 2.37×10^7 cells with a standard deviation of 6.7×10^6 cells, which corresponds to 24.5 generations. These estimates were confirmed by direct counting of the number of cells in a colony in a Petroff-Hausser counting chamber (VWR 15170-048). Due to clumping in the PHP mutant cells, a similar estimate could not be generated for these strains.

Western blots

DnaE1-MYC was detected using an anti-MYC antibody (71D10, Cell Signaling Technology) at a 1:1,000 dilution; HSP65 was detected using an anti-HSP65 antibody (BDI578, Abcam) at 1:1,000 dilution. IRDye-800 anti-mouse and IRDye-680 anti-rabbit were used at 1:15,000 dilution. Immunoblots were imaged on a Licor Odyssey scanner.

Sequencing

Genomic DNA was isolated from 10 ml *M. smegmatis* cultures using standard phenol:chloroform extraction techniques. Genomic DNA was quantified using a Qubit Fluorometer (Life Technologies) and libraries were prepared with the Illumina Nextera XT kit. Sequencing was performed using an Illumina MiSeq Desktop Sequencer with the MiSeq Reagent Kit v2. Paired-end read sequencing was performed with read lengths of 101 bases. Mutant accumulation lines were covered to an average of 74× depth (range 35× - 135×) and 96.3% genome coverage at a depth greater than 10× and mapping quality greater than or equal to 60.

SNP and INDEL calling

The reference genome was mc^{2}155, NCBI reference sequence NC_008596. Sequencing reads were aligned to the reference genome using the BWA-MEM algorithm[22]. We then applied GATK [23] base quality score recalibration, indel realignment, duplicate removal, and performed SNP and INDEL discovery and genotyping simultaneously according to GATK Best Practices recommendation[21,24]. An initial round of SNP calling on the original, non-recalibrated data was used to generate a set of "known" SNPs for use in those GATK tools that require prior SNP information. Following GATK, SNPs were filtered according to the following hard parameters (QD < 2.0 || FS > 60.0 || MQ < 50.0 || MappingQualityRankSum < −12.5 || ReadPosRankSum < −8.0).

Mutation rate estimated from MAA

The mutation rate was estimated from the number of single nucleotide polymorphisms (SNPs) and small insertions/deletions (INDELS; 10 base pairs) observed across MA lines. For the sake of simplicity, we assumed that the number of mutations (m) is an accurate assessment of the mutation rate of the strain during the course of the experiment. It is possible that the low fitness of the PHP mutant strains may disallow mildly deleterious mutations. Moreover, it is possible that the PHP mutant alleles retain a small amount of residual exonuclease activity. For these reasons, the estimate for m in the PHP mutant strains may be an underestimate. The estimation for the mutation rate for a MAA strain was generated with the equation: $\mu = m/(N*g)$. The per base pair mutation rate (μ) is determined by the number of variants m (SNPs and INDELS) divided by the covered genome size (N) times the number of generations (g). m is defined by the number of variants observed, N is determined based on 96.3% coverage of a 6,988,209 bp mc^{2}155 genome, and g is an estimate of the number of generations that occurred during passaging. Estimates of 95% confidence intervals for the mutation rate were determined using the poissfit function in Matlab (Mathworks, Natick, MA, USA).

Estimation of mutation rates by fluctuation analysis

Fluctuation analysis, *rpoB* target size determination, and statistical comparisons of fluctuation analysis data were performed as previously described[25].

Bacterial genomes and sequence data

Bacterial genome sequences (Refseq and Draft) were downloaded from NCBI (ftp.ncbi.nlm.nih.gov/genomes/). C-family DNA polymerases and epsilon exonuclease homologues were identified by performing protein sequence searches with BLAST[26] against the protein database derived from the collected bacterial genomes. BLAST searches were run until convergence (E-value = 1e-05 inclusion threshold) using the following representatives as search probes: *E. coli* DNA polymerase III alpha subunit (NP_414726.1); *B. subtilis* DNA polymerase III PolC-type (NP_389540); and *E. coli* DNA polymerase III epsilon subunit (NP_414751). If a DNA polymerase sequence contained an intein, it was excised before further analysis[19]. A small number of sequences were found fragmented, either due to frameshifts presumably as a result of sequencing/assembly errors or mis-annotation of translational start sites-such sequences were removed from further analysis. Annotated 16S rRNA sequences were extracted from Refseq and Draft bacterial genomes with custom Perl scripts. For poorly represented bacterial classes, additional sequences were identified in the nr NCBI database with BLAST. See Supplemental Table 4 for the organisms and sequences used in this study.

Multiple sequence alignments and analysis of sequence features

Sequences were parsed according to taxonomical class. Protein sequence alignments were constructed with MAFFT[27]. DNA polymerases were classified as PolC, DnaE1 (the major DNA replicative polymerase in bacteria that do not utilize PolC), or DnaEn (which includes both the DnaE2 and DnaE3 classes) based on score cutoffs from custom DNA polymerase hidden Markov models or from previous classifications[19]. For DNA polymerases, the presence of an exonuclease 'active' PHP domain was queried based on the conservation of all nine essential metal ion binding residues (HHDHEHCDH) within the PHP domain using a regular expression. DNA polymerase sequences that contained mutations within this motif were classified as having an exonuclease 'inactive' PHP domain. Classification of a subset of PolC DNA polymerases was ambiguous- these sequences conserved all nine metal ion binding residues but also had an epsilon exonuclease inserted into the PHP domain (characteristic of PolC-type DNA polymerases; see below). For this reason, such PolC sequences were classified as PHP domain exonuclease 'inactive/active?.' Sequence alignments were also used to classify epsilon homologues. An epsilon homologue was not identifiable (E-value < 1e-05) for some bacterial species. Epsilon homologues were sub-divided into one of thee categories: (1) an *E. coli*-like epsilon which we defined by the presence of a single domain protein containing a DEDDh-family exonuclease followed immediately by a clamp binding motif (Qxx[L/F/M/I]x); (2) an epsilon homolog inserted into the PHP domain of a PolC-type DNA polymerase; and (3) an epsilon homolog fused to the N-terminus of a DnaE-type DNA polymerase. *E. coli*-like epsilon homologues were further confirmed based on scoring (score cutoff > 210) as hits against the dnaQ_proteo (TIGR01406) model in the NCBI Conserved Domain Database (Supplemental Table 5)[18]. The only bacterial classes that contain *E. coli*-like epsilon exonucleases in our sequence collection (score > 210 when compared to TIGR01406) are the alpha, beta, and gammaproteobacteria (Supplemental Table 5).

Phylogenetic analysis

To facilitate phylogenetic comparison, a subset of species (8 each) from each bacterial class was chosen to represent the total organismal diversity within that class. 16S rRNA sequences were aligned with Infernal using a covarion model built from a high-quality reference alignment[28]. Initial phylogenetic relationships were constructed with FastTree with the default settings[29]. These trees were then used to guide the organism selection process based on the phylogenetic diversity (branch length), that each organism contributed to the tree. Phylogenetic trees for publication were generated with RAxML with the –f a option and the GTRGAMMA model of nucleotide substitution to generate 1000 bootstrap replicates followed by a search for the best-scoring ML tree[30]. Convergence was assessed using the –I autoMRE option in RAxML. Tree analysis and visualization were carried out with iTOL[31].

M. tuberculosis clinical strain *dnaE1* SNP analysis

M. tuberculosis genome sequences[32-34] were downloaded from repositories and converted to FASTQ files. Reads were aligned to the *M. tuberculosis* reference genome (NC_018143) with BWA-MEM[22] with the default parameters. Data was further processed using Pilon (Broad Institute) with the "--tracks" setting. SNPs within the PHP domain of DnaE1 (*Rv1547;* amino acids 1-300; genome coordinates 1747700-1748599) that passed the Pilon filtering criterion were then extracted from VCF files. A small number of samples from the Casali et al. 2014 dataset were found to be non-*M. tuberculosis* species and were excluded from the analysis.

Minimum inhibitory concentration (MIC) determination

MIC determination was performed as previously described[35].

Protein expression and purification

M. tuberculosis dnaE1 (Rv1547) was cloned into the pYUB28b vector (kindly provided by Edward Baker, University of Auckland, New Zealand) and transformed into electro-competent *Mycobacterium smegmatis* mc^{2}4517 (kindly provided by William Jacobs, Albert Einstein College of Medicine, United States). Cells were grown in ZYP-5052 culture medium[36] at 37°C and 200 rpm, harvested at $0D_{600}$=6.0 and stored at −80°C. Wild-type and mutant DnaE1^{MTB} were purified using nickel affinity, anion exchange and gel filtration columns and his-tags were cleaved with HRV 3C protease. All purification steps were done in 50 mM HEPES pH 7.5, 0.1-1.0 M NaCl and 2 mM DTT. Proteins were stored at −80°C in 50 mM HEPES pH 7.5, 150 mM NaCl and 2 mM DTT. *E. coli* PolIIIα and ε were purified as described previously from BL21 DE3 *E. coli*[37]. To remove trace amounts of co-purifying endogenous exonuclease, PolIIIα was incubated with an excess ε peptide (residues 209 – 243) and purified using gel filtration.

Polymerase and exonuclease assays

All assays were performed in 50 mM HEPES pH 7.5, 50 mM potassium glutamate, 6 mg/ml BSA, 2 mM DTT and 2 mM magnesium acetate. Real-time primer extension assays were performed as described previously[37], using 23 nM protein, 216 nM unlabeled DNA, 21.6

nM labeled DNA, and 4 μM dGTP. To determine V_{max} and K_m of DnaE1[MTB] and PolIIIα[EC], incorporation rates were measured at 0-100 μM dGTP and data fitted in Graphpad Prism (Version 6 for Mac OSX, Graphpad Software, San Diego, CA, USA) using the results from three independent experiments. For gel analysis, reactions were performed at 22°C with 6 nM purified protein and 100 nM DNA substrate. Primer extensions were done for 5 minutes in the presence of 100 μM dNTP unless stated otherwise. For inhibition assays, 200 μM Adenine-arabinofuranoside-5′-triphosphate (ara-A; Jena Bioscience) were added to the reaction. For exonuclease assays, samples were taken at different time points. Reactions were stopped in 50 mM EDTA pH 7.4, separated on a denaturing 20% acrylamide gel and imaged with a Typhoon Imager (GE Healthcare).

Size exclusion chromatography

50 μl samples of the purified proteins were prepared at 10 μM and injected onto a Superdex 200 Increase 3.2/300 gel filtration column (GE Healthcare) pre-equilibrated in 50 mM HEPES pH 7.5, 150 mM NaCl and 2 mM DTT.

DNA substrates

DNA oligos were purchased from Integrated DNA Technologies (sequences shown in Supplemental Table 6). 6-FAM labeled oligos were purified using a denaturing 20% acrylamide gel. Substrates were annealed in a 3× excess of unlabelled oligo and stored in 10 mM Tris-HCl pH 8.0 and 1 mM EDTA at −20°C.

Circular Dichroism (CD) and thermal melt

CD scans (185-260 nm) were performed in 10 mM KH_2PO_4 pH 7.0, 100 mM KF and 1 mM DTT with a Jasco J-815 instrument using 200 μL of 1 μM dialyzed protein at 20°C. Following this, the protein samples were subjected to a thermal melt increasing to 90°C with steps of 1 degrees/min. Structural changes were monitored at 222 nm.

Modeling of the DnaE1[MTB] PHP domain

The model of the DnaE1[MTB] PHP domain was created using the program Modeller[38] using the crystal structure of *Taq* PolIIIα[39] as a template. For this, a sequence alignment of DnaE1[MTB] and *T. aquaticus* PolIIIα was calculated with Clustal[40] and ESPript[41] using multiple DnaE1 and PolIIIα sequences from different bacterial species. Figures were prepared with PyMol (The PyMOL Molecular Graphics System, Version 1.5.0.4 Schrödinger, LLC.).

Supplementary Material

Refer to Web version on PubMed Central for supplementary material.

Acknowledgements

References

1. Robinson A, Causer RJ, Dixon NE. Architecture and conservation of the bacterial DNA replication machinery, an underexploited drug target. Curr Drug Targets. 2012; 13:352–372. [PubMed: 22206257]

2. Kunkel TA, Bebenek K. DNA Replication Fidelity. Annu. Rev. Biochem. 2000; 69:497–529. [PubMed: 10966467]

3. Mizrahi V, Andersen SJ. DNA repair in Mycobacterium tuberculosis. What have we learnt from the genome sequence? Molecular Microbiology. 1998; 29:1331–1339. [PubMed: 9781872]

4. Springer B, et al. Lack of mismatch correction facilitates genome evolution in mycobacteria. Molecular Microbiology. 2004; 53:1601–1609. [PubMed: 15341642]

5. Ford CB, et al. Use of whole genome sequencing to estimate the mutation rate of Mycobacterium tuberculosis during latent infection. Nat Genet. 2011; 43:482–486. [PubMed: 21516081]

6. Farhat MR, et al. Genomic analysis identifies targets of convergent positive selection in drug-resistant Mycobacterium tuberculosis. Nat Genet. 2013; 45:1183–1189. [PubMed: 23995135]

7. Cole ST, et al. Massive gene decay in the leprosy bacillus. Nature. 2001; 409:1007–1011. [PubMed: 11234002]

8. McHenry CS. DNA replicases from a bacterial perspective. Annu. Rev. Biochem. 2011; 80:403–436. [PubMed: 21675919]

9. Stano NM, Chen J, McHenry CS. A coproofreading Zn(2+)-dependent exonuclease within a bacterial replicase. Nat. Struct. Mol. Biol. 2006; 13:458–459. [PubMed: 16604084]

10. Wing RA, Bailey S, Steitz TA. Insights into the Replisome from the Structure of a Ternary Complex of the DNA Polymerase III α-Subunit. Journal of Molecular Biology. 2008; 382:859–869. [PubMed: 18691598]

11. Barros T, et al. A structural role for the PHP domain in E. coli DNA polymerase III. BMC Struct Biol. 2013; 13:8. [PubMed: 23672456]

12. Sassetti CM, Boyd DH, Rubin EJ. Comprehensive identification of conditionally essential genes in mycobacteria. Proc Natl Acad Sci USA. 2001; 98:12712–12717. [PubMed: 11606763]

13. Malshetty VS, Jain R, Srinath T, Kurthkoti K, Varshney U. Synergistic effects of UdgB and Ung in mutation prevention and protection against commonly encountered DNA damaging agents in Mycobacterium smegmatis. Microbiology. 2010; 156:940–949. [PubMed: 19942658]

14. Lee H, Popodi E, Tang H, Foster PL. Rate and molecular spectrum of spontaneous mutations in the bacterium Escherichia coli as determined by whole-genome sequencing. Proc Natl Acad Sci USA. 2012; 109:E2774–83. [PubMed: 22991466]

15. Fijalkowska IJ, Schaaper RM. Mutants in the Exo I motif of Escherichia coli dnaQ: defective proofreading and inviability due to error catastrophe. Proc Natl Acad Sci USA. 1996; 93:2856–2861. [PubMed: 8610131]

16. Denamur E, Matic I. Evolution of mutation rates in bacteria. Molecular Microbiology. 2006; 60:820–827. [PubMed: 16677295]

17. Dalrymple BP, Kongsuwan K, Wijffels G, Dixon NE, Jennings PA. A universal protein-protein interaction motif in the eubacterial DNA replication and repair systems. Proc Natl Acad Sci USA. 2001; 98:11627–11632. [PubMed: 11573000]

18. Haft DH, et al. TIGRFAMs: a protein family resource for the functional identification of proteins. Nucleic Acids Research. 2001; 29:41–43. [PubMed: 11125044]

19. Timinskas K, Balvo i t M, Timinskas A, Venclovas . Comprehensive analysis of DNA polymerase III α subunits and their homologs in bacterial genomes. Nucleic Acids Res. 2014; 42:1393–413. [PubMed: 24106089]

20. Jordheim LP, Durantel D, Zoulim F, Dumontet C. Advances in the development ofnucleoside and nucleotide analoguesfor cancer and viral diseases. Nat Rev Drug Discov. 2013; 12:447–464. [PubMed: 23722347]

21. Long MC, et al. Structure-activity relationship for adenosine kinase from Mycobacterium tuberculosis. Biochem. Pharmacol. 2008; 75:1588–1600. [PubMed: 18329005]

Methods References

22. Li H, Durbin R. Fast and accurate short read alignment with Burrows-Wheeler transform. Bioinformatics. 2009; 25:1754–1760. [PubMed: 19451168]

23. McKenna A, et al. The Genome Analysis Toolkit: a MapReduce framework for analyzing next-generation DNA sequencing data. Genome Res. 2010; 20:1297–1303. [PubMed: 20644199]

24. DePristo MA, et al. A framework for variation discovery and genotyping using next-generation DNA sequencing data. Nat Genet. 2011; 43:491–498. [PubMed: 21478889]

25. Ford CB, et al. Mycobacterium tuberculosis mutation rate estimates from different lineages predict substantial differences in the emergence of drug-resistant tuberculosis. Nat Genet. 2013; 45:784–790. [PubMed: 23749189]

26. Altschul SF, Gish W, Miller W, Myers EW, Lipman DJ. Basic local alignment search tool. Journal of Molecular Biology. 1990; 215:403–410. [PubMed: 2231712]

27. Katoh K, Misawa K, Kuma K-I, Miyata T. MAFFT: a novel method for rapid multiple sequence alignment based on fast Fourier transform. Nucleic Acids Res. 2002; 30:3059–3066. [PubMed: 12136088]

28. Nawrocki EP, Eddy SR. Infernal 1.1: 100-fold faster RNA homology searches. Bioinformatics. 2013; 29:2933–2935. [PubMed: 24008419]

29. Price MN, Dehal PS, Arkin AP. FastTree 2--approximately maximum-likelihood trees for large alignments. PLoS ONE. 2010; 5:e9490. [PubMed: 20224823]

30. Stamatakis A. RAxML version 8: a tool for phylogenetic analysis and post-analysis of large phylogenies. Bioinformatics. 2014; 30:1312–1313. [PubMed: 24451623]

31. Letunic I, Bork P. Interactive Tree Of Life v2: online annotation and display of phylogenetic trees made easy. Nucleic Acids Res. 2011; 39:W475–W478. [PubMed: 21470960]

32. Casali N, et al. Evolution and transmission of drug-resistant tuberculosis in a Russian population. Nat Genet. 2014; 46:279–286. [PubMed: 24464101]

33. Zhang H, et al. Genome sequencing of 161 Mycobacterium tuberculosis isolates from China identifies genes and intergenic regions associated with drug resistance. Nat Genet. 2013; 45:1255–1260. [PubMed: 23995137]

34. Comas I, et al. Out-of-Africa migration and Neolithic coexpansion of Mycobacterium tuberculosis with modern humans. Nat Genet. 2013; 45:1176–1182. [PubMed: 23995134]

35. Franzblau SG, et al. Rapid, low-technology MIC determination with clinical Mycobacterium tuberculosis isolates by using the microplate Alamar Blue assay. Journal of Clinical Microbiology. 1998; 36:362–366. [PubMed: 9466742]

36. Studier FW. Protein production by auto-induction in high-density shaking cultures. Protein Expression and Purification. 2005; 41:207–234. [PubMed: 15915565]

37. Toste Rêgo A, Holding AN, Kent H, Lamers MH. Architecture of the Pol III-clamp-exonuclease complex reveals key roles of the exonuclease subunit in processive DNA synthesis and repair. EMBOJ. 2013; 32:1334–1343.

38. Eswar N, et al. Comparative protein structure modeling using MODELLER. Curr Protoc Protein Sci. 2007 Chapter 2, Unit 2.9.

39. Bailey S, Wing RA, Steitz TA. The Structure of T. aquaticus DNA Polymerase III Is Distinct from Eukaryotic Replicative DNA Polymerases. Cell. 2006; 126:893–904. [PubMed: 16959569]

40. Larkin MA, et al. Clustal W and Clustal X version 2.0. Bioinformatics. 2007; 23:2947–2948. [PubMed: 17846036]

41. Gouet P. ESPript/ENDscript: extracting and rendering sequence and 3D information from atomic structures of proteins. Nucleic Acids Res. 2003; 31:3320–3323. [PubMed: 12824317]
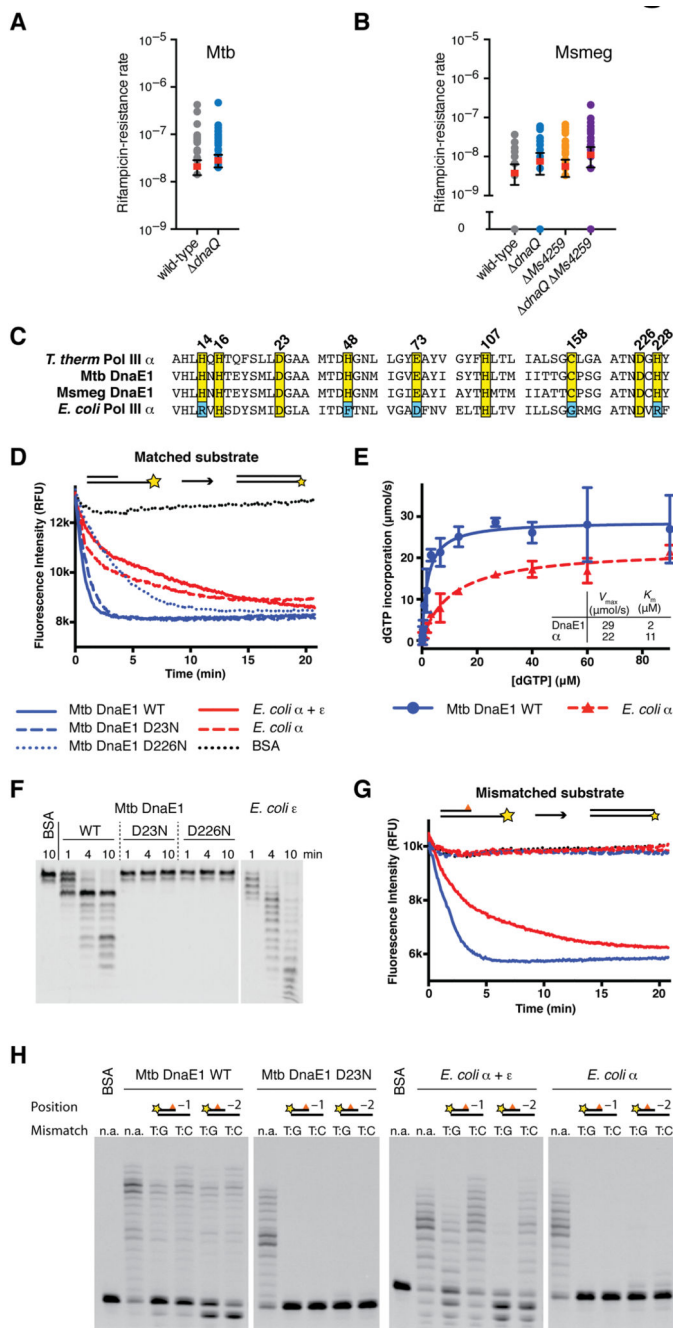
Figure 1. The *M. tuberculosis* DnaE1 polymerase encodes an intrinsic proofreading capability
(A) Rates at which the indicated *M. tuberculosis* strains acquired resistance to rifampicin were measured by fluctuation analysis. *Rv3711c* is the annotated *dnaQ* gene. Circles represent mutant frequency (number of rifampicin-resistant mutants per cell plated in a single culture). Red bars represent the estimated mutation rates (mutations conferring rifampicin resistance per generation), with error bars representing the 95% confidence intervals.

(B) Fluctuation analysis was performed with the indicated *M. smegmatis* strains as in Figure 1A. *Ms6275* is the annotated *dnaQ* gene and *Ms4259* is next closest *dnaQ* homologue.

(C) Alignment of DNA polymerase PHP domains from the indicated species.

(D) Real-time primer extension activity of purified polymerases. Primer extension results in quenching of template fluorophore.

(E) V_{max} and K_m measurements derived from three primer extension assays. DnaE1^{MTB} incorporates nucleotides faster than PolIIIα^{EC}. Data points indicate the mean and error bars the standard deviation.

(F) Time course of 3′-5′ exonuclease activity on ssDNA. Wild-type DnaE1^{MTB} shows robust exonuclease activity while the PHP mutants D23N & D226N do not. Note the distinct digestion patterns of DnaE1^{MTB} and ε^{EC}-exonuclease.

(G) Primer extension assay as in Figure 2B with a mismatched DNA substrate. Exonuclease deficient polymerases cannot extend from mismatched DNA, while wild-type DnaE1^{MTB} and PolIIIα^{EC}+ε^{EC} activities are unaffected.

(H) Gel analysis of primer extension reactions shows that extension from mismatched primers requires exonuclease activity, while extension activity on matched substrates (n.a.) is unaffected.
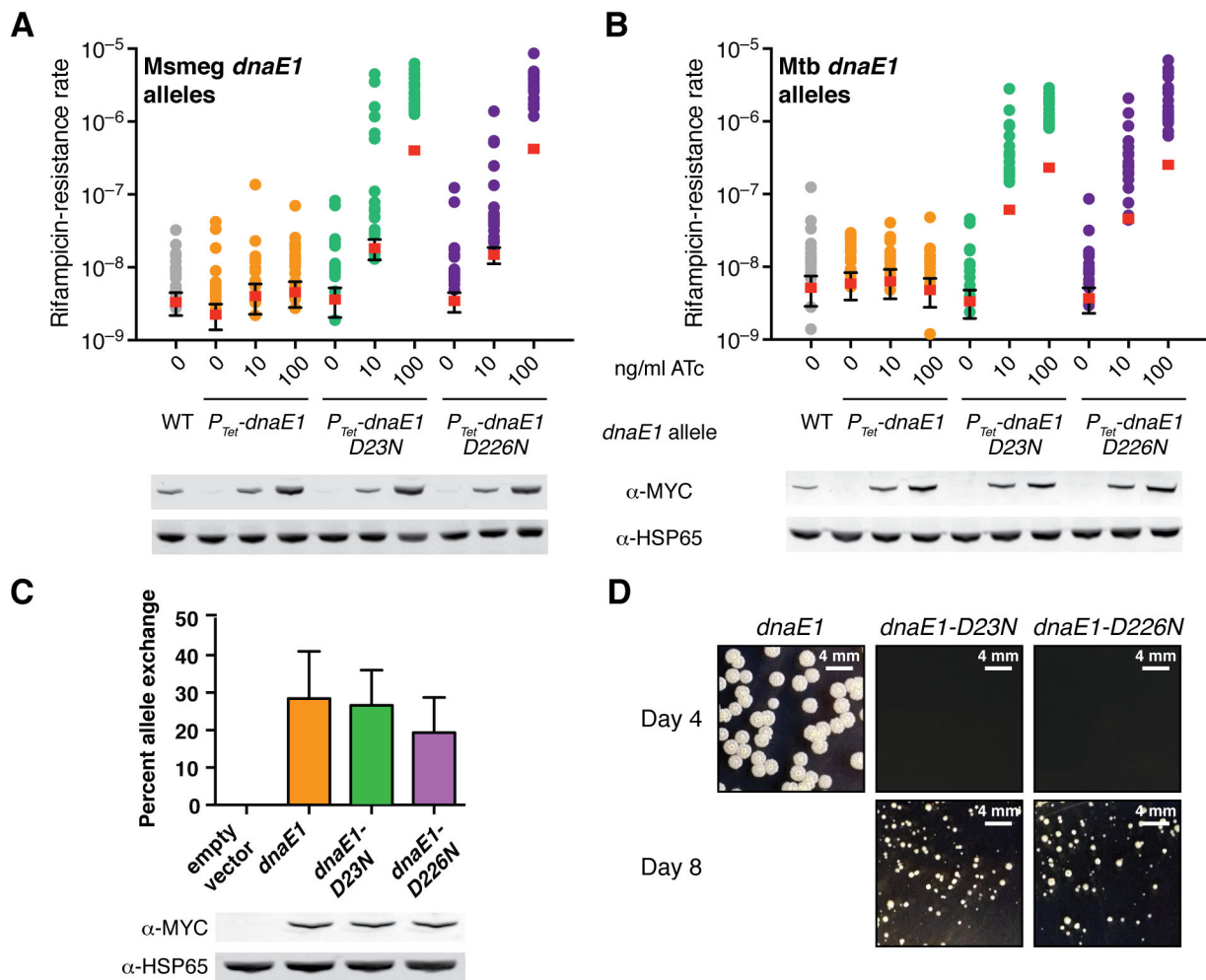
Figure 2. Inactivation of DnaE1 proofreading results in a mutator phenotype *in vivo*

(A-B) Fluctuation analysis in *M. smegmatis* was performed as in Figure 1A. The indicated strains have both the wild-type endogenous *dnaE1* allele as well as an anhydrotetracycline (ATc) regulated *dnaE1* allele integrated at the *L5 attB* site. To enable comparison of protein levels, a MYC-tagged *dnaE1* allele under the control of its endogenous promoter was loaded under the "WT" lane. For the sake of simplicity, DnaE1^{MTB} numbering was used throughout the paper.

(C) Allele-exchange experiment in a Δ*dnaE1 dnaE1::attB(L5) M. smegmatis* strain. Plasmids carrying the indicated MYC-tagged *dnaE1* alleles were tested for the ability to exchange for the resident *attB*-integrated plasmid in the parent strain. Error bars indicate standard deviation from three experiments.

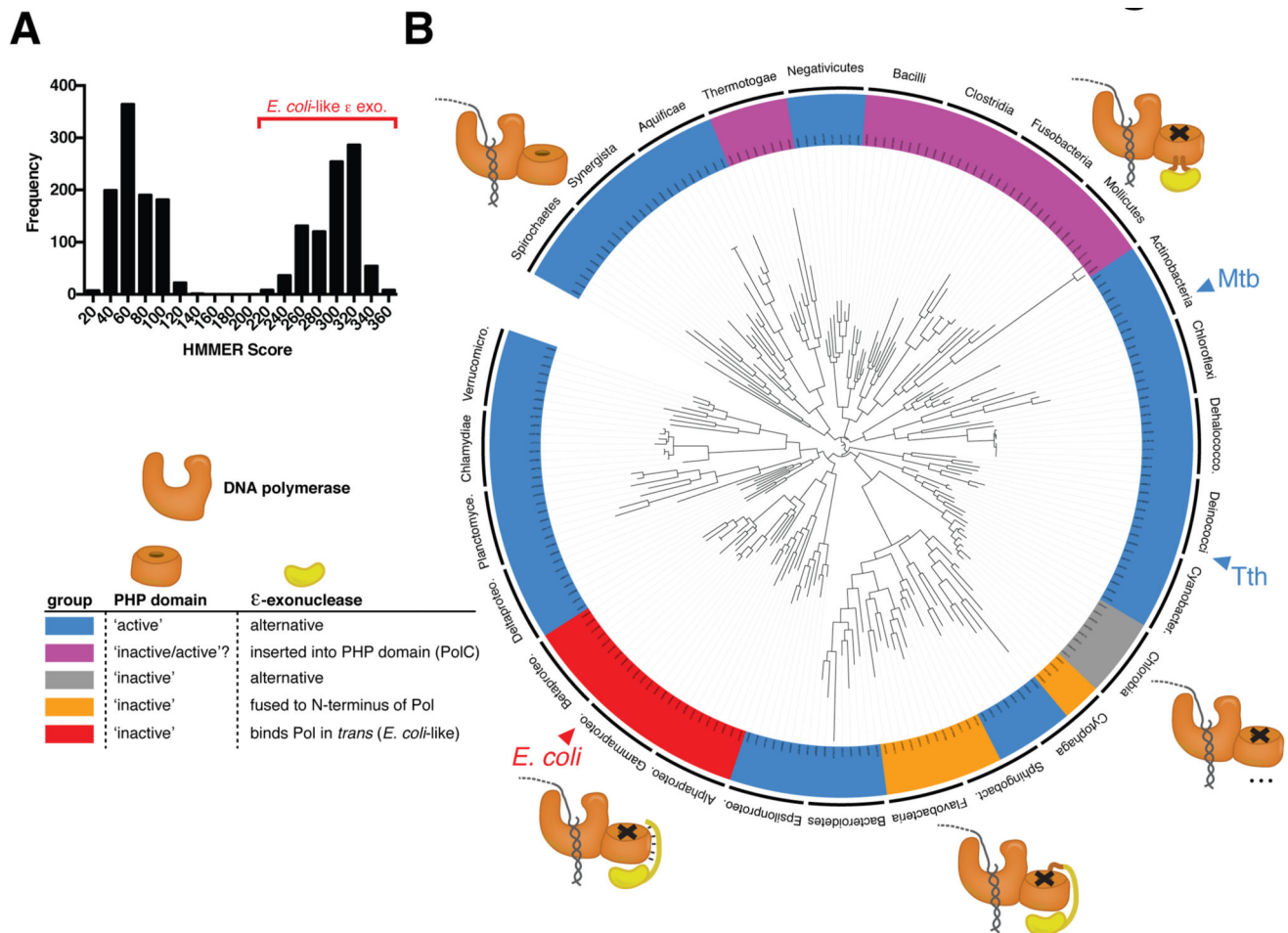(D) Growth of indicated *M. smegmatis* strains.

Figure 3. Conservation of PHP domain-mediated DNA replication proofreading

(A) ε-exonuclease homologues identified by BLAST were compared to the *E.coli*-like ε-exonuclease dnaQ_proteo (TIGR01406) HMM model. The distribution of scores is shown. (B) Bacterial phylogenetic tree inferred from an alignment of 16S rRNA genes using RAxML. Subsets of eight species from each bacterial class (labeled on the outer ring of the tree) were chosen to represent the total organismal diversity within each class. Species are colored along the outer ring according to the legend as indicated. A subset of PolC containing bacteria (purple strip) have PolC polymerases that have conserved all nine PHP domain metal ion binding residues in addition to having an ε-exonuclease inserted into the PHP domain. For this reason, the PolC containing bacteria have been labeled ['inactive/active'?].
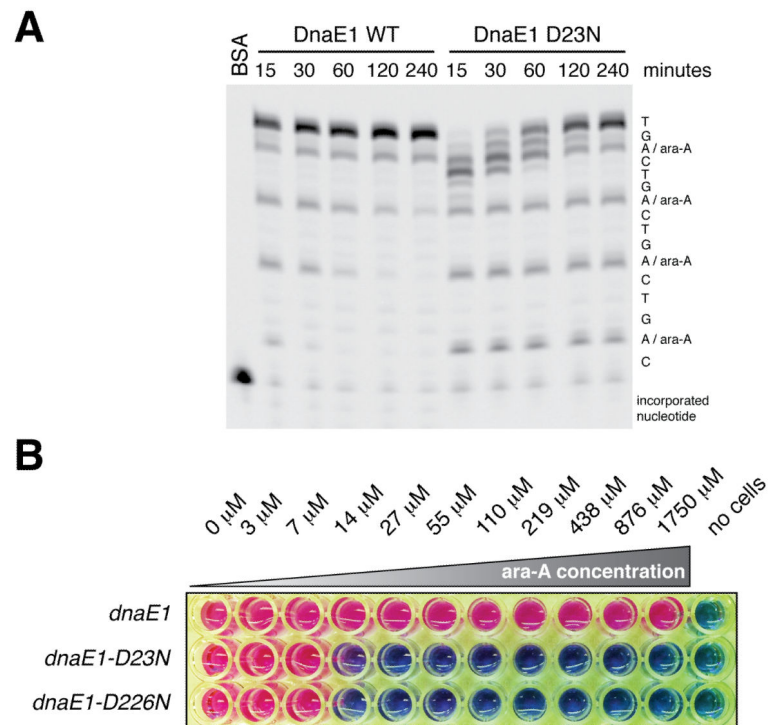
Figure 4. Inactivation of the PHP domain renders mycobacteria sensitive to nucleoside analogues
(A) Primer extension analysis performed as in Figure 1H in the presence of 200 μM of the adenosine analog ara-A. Incorporation of ara-A impedes primer extension. Whereas wild-type DnaE1^{MTB} can excise ara-A and resume DNA synthesis, the PHP mutants cannot.
(B) Determination of the minimum inhibitory concentration (MIC) of ara-A for the indicated *M. smegmatis* strains. Pink color indicates cellular respiration; blue color indicates lack of respiration.

Table 1

Estimation of mutation rates by mutant accumulation assay. Mutations are classified according to base pair substitutions (BPSs) or indels (defined here as insertions or deletions ≥ 10 nucleotides). CI = confidence interval.

Strain	No. of BPSs	No. of indels	No. of lines	Total no. of generations	Mutation rate per base pair	95% CI	Mutation rate per genome	95% CI
dnaE1	9	7	6	5,250	4.52×10^{-10}	$(2.59–7.35) \times 10^{-10}$	3.0×10^{-3}	$(1.7–4.9) \times 10^{-3}$
dnaE1-D23N	5,751	1,860	11	1,100	1.03×10^{-6}	$(1.00–1.05) \times 10^{-6}$	6.9	6.8–7.1
dnaE1-D226N	10,269	2,265	11	1,100	1.69×10^{-6}	$(1.66–1.73) \times 10^{-6}$	11.4	11.2–11.6